33rd Annual International Conference of the IEEE EMBS
Boston, Massachusetts USA, August 30 - September 3, 2011

Effect of White Matter Anisotropy in Modeling Electroconvulsive Therapy

Siwei Bai, *Student Member*, *IEEE*, Colleen Loo, Guangqiang Geng, and Socrates Dokos, *Member*, *IEEE*

***Abstract*— White matter in the brain exhibits strong anisotropic conductivity. Modeling studies on electroencephalography have found that such anisotropic conductivity greatly influences the estimated dipole source. In this study, we made a detailed comparison of the effects of conductivity anisotropy using a computational model of electroconvulsive therapy (ECT). The human head model was a high resolution finite element model generated from MRI scans, implemented with tissue heterogeneity and an excitable neural model incorporated in the brain. Results showed that anisotropy in conductivity had minimal effects on the location of the brain region that was maximally activated, but it had relatively large effects on deep brain structures.**

I. Introduction

White matter (WM) in the brain is known to exhibit highly anisotropic electrical conductivity [1], [2], as water molecules and ions inside nerve fibres can flow more easily along the fibre tracts than transverse to them. Following the assumption that the electric conductivity tensor shares the same eigenvalues as the water diffusion tensor [3], the latter can be measured by diffusion tensor magnetic resonance imaging (DT-MRI). The linear relationship between the conductivity tensor and diffusion tensor has been experimentally validated [4], [5].

Modeling studies on electroencephalography (EEG) suggest that such anisotropic conductivity greatly influences the estimated dipole source [6]–[9]. Hence, WM with conductivity anisotropy should be incorporated in computational models of the head whenever possible. Although several simulation studies on transcranial stimulation have modeled WM with anisotropic conductivity [10]–[13], a detailed comparison of the effects of WM anisotropy on brain activation is still missing.

The objective of this study was to validate the effect of WM conductivity anisotropy by comparing isotropic and anisotropic computational ECT models. In this study, a finite element (FE) model of the human head based on magnetic resonance imaging (MRI) was used, with an excitable neural model incorporated in the brain.

S. Bai and S. Dokos are with Graduate School of Biomedical Engineering, Faculty of Engineering, University of New South Wales (UNSW), Australia. C. Loo is with School of Psychiatry, UNSW, Department of Psychiatry, St George Hospital and the Black Dog Institute, Australia. G. Geng is with Neuroscience Research Australia, Australia. Email:s.bai@student.unsw.edu.au; colleen.loo@unsw.edu.au; j.geng@neura.edu.au; s.dokos@unsw.edu.au.

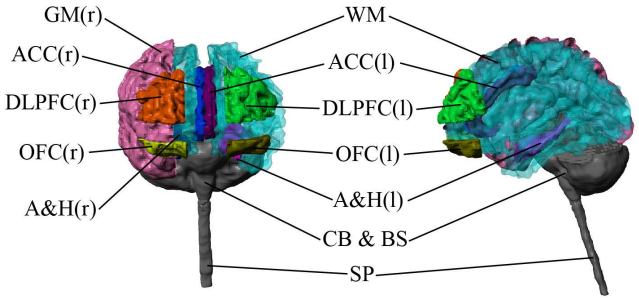

Fig. 1. Detailed segmentation of the brain, including defined regions for white matter (WM), grey matter (GM), anterior cingulate cortex, (ACC), dorsolateral prefrontal cortex (DLPFC), orbitofrontal cortex (OFC), amygdala and hippocampus (A&H), cerebellum (CB), brainstem (BS), and cervical spinal cord (SP). 'l' and 'r' denote left and right sides of the brain respectively.

II. Methods

A. Image segmentation and finite element mesh generation

T1-weighted MR imaging of a healthy 35-year-old Asian male subject was obtained from Neuroscience Research Australia. The scan resolution was 1 mm in every direction.

The head tissue masks were obtained with BrainSuite2 (www.loni.ucla.edu/Software/BrainSuite) [14] for initial automated segmentation, and ScanIP (Simpleware Ltd., UK) for manual correction and further segmentation. Later, to increase computational efficiency, the images were downsampled to a resolution of $1.5 \times 1.5 \times 1.5$ mm^3. Several regions of interest (ROIs) in the brain considered important in ECT therapeutic or adverse effects were manually segmented, including the dorsolateral prefrontal cortex (DLPFC), orbitofrontal cortex (OFC), anterior cingulate cortex (ACC), amygdala and hippocampus (A&H), as shown in Fig. 1.

The +FE-Free meshing algorithm in ScanIP was chosen to generate the mesh. The resulting mesh model consisted of 1,126,135 elements.

B. White matter conductivity anisotropy

DT-MRI was performed on the same subject in 61 directions. The slices were axially oriented with voxel resolution of $2.5 \times 2.5 \times 2.5$ mm^3. After registration to the structural scans, the images were imported in FSL (www.fmrib.ox.ac.uk/fsl/index.html) for diffusion tensor calculation, which was performed using probabilistic tracking algorithm in the software's diffusion toolbox FDT [15]–[17]. Eigenvectors and fractional anisotropy (FA) were then

TABLE I

TISSUE CONDUCTIVITIES

Compartment	Electrical Conductivity (S/m)
Scalp	0.41
Eye	0.5
Sinus (air-filled)	0
Skull (spongy bone)	0.028
Skull (compact bone)	0.006
Vertebrae	0.012
CSF	1.79
Brain (except WM)	0.31
WM (isotropic)	0.14
WM (longitudinal)	0.65
WM (transverse)	0.065

TABLE II

AVERAGE E-FIELD (V/M) IN ROIS BETWEEN MODELS WITH AND WITHOUT WHITE MATTER ANISOTROPY

Compartment	E-field (V/m)		% Difference
	with Anisotropy	without Anisotropy	(relative to isotropic case)
whole brain	28.5	27.4	4.1%
DLPFC	42.8	41.0	4.6%
OFC	55.0	46.4	18.4%
ACC	11.4	6.82	67.3%
A&H	25.7	19.9	29.0%

calculated: the latter being widely used to denote the degree of anisotropy and is typically greater than 0.45 for WM [18]. Figs. 2a and 3a show the FA maps (before and after threshold) of an axial and coronal slice in the brain.

The conductivity tensor σ for WM was calculated from:

$$\boldsymbol{\sigma} = \mathbf{S}\,\mathrm{diag}(\sigma_l, \sigma_t, \sigma_t)\,\mathbf{S}^T, \tag{1}$$

where $\mathbf{S}$ is the orthogonal matrix of unit eigenvectors of the diffusion tensor, and σ_l and σ_t are the conductivities longitudinal and transverse to the fibre directions respectively, with $\sigma_l : \sigma_t = 10 : 1$ [2], [19]. σ_l and σ_t were calculated using a volume constraint [9], which retained the geometric mean of eigenvalues and thus the 'volume' of the conductivity tensor, i.e.

$$\frac{4}{3}\pi\sigma_l\sigma_t^2 \equiv \frac{4}{3}\pi\sigma_{\mathrm{iso}}^3, \tag{2}$$

where σ_{iso} is the generic isotropic WM conductivity. Only fibre conductivities with strong anisotropy signal (FA ≥ 0.45) were calculated.

C. Tissue properties

Head compartment conductivities, listed in Table I, were based on experimental data from the literature [1], [20]–[23]. The conductivity of brain (except WM) was assigned to all grey matter (GW) regions, as well as the cerebellum (CB) and spinal cord (SC).

D. Field solver for volume conductors

ECT electrodes were defined mathematically on the scalp, as described in Bai *et al*. [24]. The electrode configuration used was bitemporal (BT), i.e. two bilateral electrodes placed 3 cm superior to the midpoint of a line on each side of the head connecting the external ear canal with the lateral angle of the eye. The electrode stimulus current was a single monophasic square pulse of amplitude 800 mA and pulsewidth 1 ms, with the left electrode being the anode and right electrode the cathode.

Brain compartments including GM, WM and CB were simulated using a modified bidomain ionic continuum model based on the Hodgkin-Huxley formulation [25]. Remaining head compartments were simulated as passive volume conductors. Detailed descriptions of the model can be found in Bai *et al*. [24].

When implemented, both the anisotropic and isotropic WM models had more than 6×10^6 degrees of freedom. They were solved using COMSOL Multiphysics (COMSOL AB, Sweden) finite element software using a segregated numerical solver on a Windows 64-bit workstation with 24 GB RAM utilizing 4 processors. To solve the time-dependent equations, a variable step backward differentiation formula (BDF) scheme was utilized with an absolute error tolerance set to 10^{-3}. It took approximately 20 hours to solve for a 6-millisecond simulation.

III. RESULTS

Figs. 2b and 2c compare the electric field magnitude (E-field) and the maximal spatial extent of brain activation between models with and without WM anisotropy in an axial slice across the temporal lobe. Figs. 3b and 3c also plot these in a coronal slice through the temporal lobe. The comparison in E-field demonstrates that both models exhibited maximal electric fields in the regions immediately adjacent to the electrodes. The E-field in the anisotropic model exhibited inhomogeneous regions of greater electric field concentration compared to the isotropic case where the electric field was slightly more uniform and diffuse. In addition, the directionality of the E-field in the anisotropic model also largely agreed with the FA map after threshold (Fig. 2a and 3a). On the other hand, the comparison in excitation reveals that there was only a small difference in the spatial extent of brain regions that were maximally excited.

Table 2 shows the comparison in average E-field among ROIs in the isotropic and anisotropic models. From the table, it is evident that the average E-fields in the whole brain and in DLPFC exhibited minimal difference, both less than 5%; while the difference in the ACC region was maximal at greater than 50%.

IV. DISCUSSION

This study demonstrates the effect of WM electrical anisotropy in transcranial stimulation by comparing BT ECT models with and without anisotropic conductivity. Both the distribution of E-fields and the spatial extent of brain activation were examined. The major advantage of including neuronal activation in our model, is that it allows the investigation additional effects such as altered stimulus pulsewidth on brain activation. If desired, our approach can also be

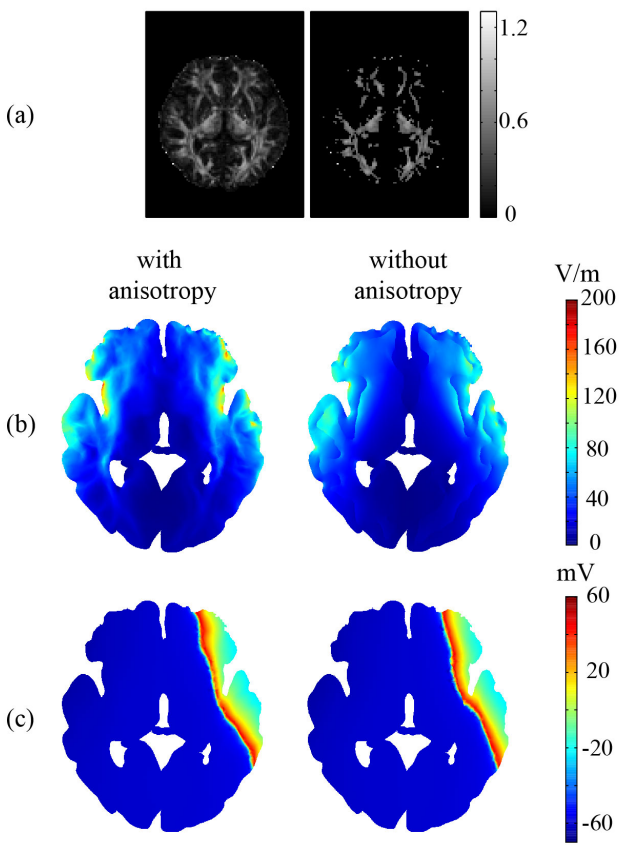

Fig. 2. Results in an axial slice across the temporal lobe. a): FA map before and after threshold (FA $\geq$ 0.45); b): E-field distribution in the brain; c): maximum spatial extent of brain excitation, shown as neuronal membrane potential plot.

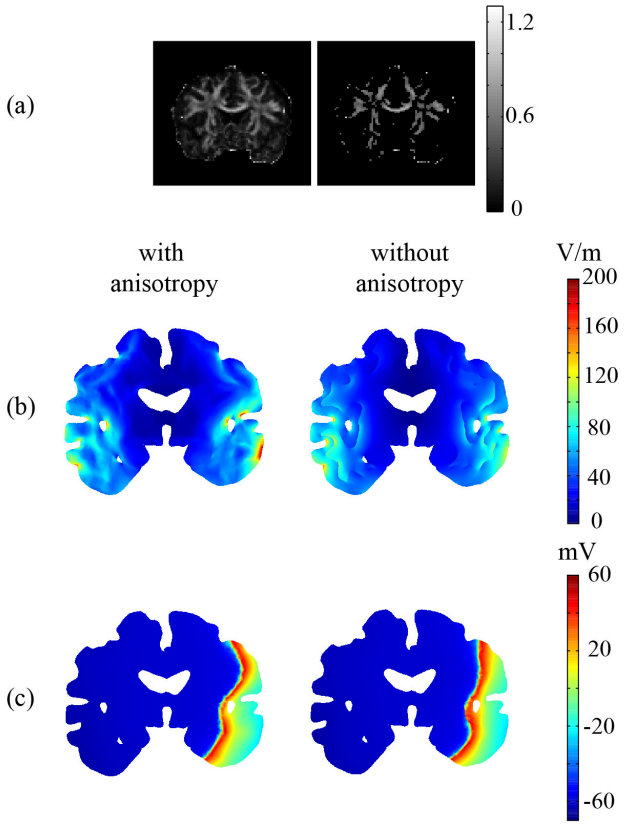

Fig. 3. Results in a coronal slice across the temporal lobe. a): FA map before and after threshold (FA $\geq$ 0.45); b): E-field distribution in the brain; c): maximum spatial extent of brain excitation, shown as neuronal membrane potential plot.

extended to investigate the dynamic effects of longer stimulus trains or even transcranial DC stimulation.

The strength of the E-field was found to be of same order of magnitude as those in existing studies, while the spatial profile slightly varied [11], [26]. This was likely due to the non-zero current source arising from the neuronal elements within the brain that contributed to the electric field in our model [24].

Since a similar overall WM conductivity resulted from the 'volume constraint' algorithm [9], the average E-field in the entire brain exhibited only a minor difference between the isotropic and anisotropic models. On the other hand, the E-field in the DLPFC also exhibited a small difference, likely due to the fact that DLPFC, mostly GM, lies on the lateral surface of the brain, and thus it was minimally influenced by the WM anisotropy. However, the further below the cortical surface, the greater the anisotropy influence was shown, and hence the greater the difference was seen. Therefore, deep brain structures were more likely affected by the WM anisotropy. A similar conclusion was also drawn from an existing comparison study on transcranial magnetic stimulation (TMS) [10]. Furthermore, even though OFC is also cortical GM, the relative difference was still high compared to DLPFC, likely due to its longer distance from the electrode. Therefore, electrode placement may also add to the complex influence of anisotropy.

In addition, since direct brain activation was mainly focused on the cortex, the influence of WM anisotropy was not prominent: the influence was revealed only when the excitation reached deep regions. An additional reason for the small difference in brain activation is that our continuum model did not incorporate neuronal orientation and connectivity. A revised model implemented with connections between neurons also has the potential to model the seizure; however, it will also be extremely computationally demanding.

As noted in Bai *et al.* [24], the parameters of our model were adjusted based on limited imaging studies [27], [28]. It is therefore highly desirable to undertake additional imaging experiments to further refine and develop our 3D model of brain activation.

V. Conclusion

This study investigated the effect of WM anisotropic conductivity on transcranial current stimulation using a high resolution finite element model generated from MRI scans, implemented with tissue heterogeneity and excitable neuronal model incorporated in the brain. Our results showed

that the electric field distribution as well as the spatial extent of brain activation remained relatively unchanged in both isotropic and anisotropic models, while activation in particular deep brain structures was variable. These results suggest that WM conductivity anisotropy plays an important role in activation of deep brain structures, and such anisotropy should be incorporated into computational head models of transcranial stimulation wherever possible.

VI. Acknowledgment

The authors would like to thank Neuroscience Research Australia for their support in acquiring and processing the structural MRI and DT-MRI data.

References

[1] L. A. Geddes and L. E. Baker, "The specific resistance of biological material - a compendium of data for the biomedical engineer and physiologist," *Medical and Biological Engineering and Computing*, vol. 5, no. 3, pp. 271–293, 1967.

[2] P. Nicholson, "Specific impedance of cerebral white matter," *Experimental Neurology*, vol. 13, no. 4, pp. 386–401, 1965.

[3] P. Basser, J. Mattiello, and D. LeBihan, "MR diffusion tensor spectroscopy and imaging," *Biophysical Journal*, vol. 66, no. 1, pp. 259–267, 1994.

[4] S. Oh, S. Lee, M. Cho, T. Kim, and I. Kim, "Electrical conductivity estimation from diffusion tensor and T2: a silk yarn phantom study," in *Proceedings of the International Society for Magnetic Resonance in Medicine*, vol. 14, pp. 3034, 2006.

[5] D. Tuch, V. Wedeen, A. Dale, J. George, and J. Belliveau, "Conductivity tensor mapping of the human brain using diffusion tensor MRI," *Proceedings of the National Academy of Sciences of the United States of America*, vol. 98, no. 20, p. 11697, 2001.

[6] H. Hallez, P. Van Hese, B. Vanrumste, P. Boon, Y. D'Asseler, I. Lemahieu, and R. Van de Walle, "Dipole localization errors due to not incorporating compartments with anisotropic conductivities: simulation study in a spherical head model," *International Journal of Bioelectromagnetism*, vol. 7, no. 1, pp. 134–137, 2005.

[7] J. Haueisen, D. Tuch, C. Ramon, P. Schimpf, V. Wedeen, J. George, and J. Belliveau, "The influence of brain tissue anisotropy on human EEG and MEG," *NeuroImage*, vol. 15, no. 1, pp. 159–166, 2002.

[8] M. Rullmann, A. Anwander, M. Dannhauer, S. Warfield, F. Duffy, and C. Wolters, "EEG source analysis of epileptiform activity using a 1 mm anisotropic hexahedra finite element head model," *NeuroImage*, vol. 44, no. 2, pp. 399–410, 2009.

[9] C. H. Wolters, A. Anwander, X. Tricoche, D. Weinstein, M. A. Koch, and R. S. MacLeod, "Influence of tissue conductivity anisotropy on EEG/MEG field and return current computation in a realistic head model: a simulation and visualization study using high-resolution finite element modeling," *NeuroImage*, vol. 30, no. 3, pp. 813–826, 2006.

[10] M. De Lucia, G. Parker, K. Embleton, J. Newton, and V. Walsh, "Diffusion tensor MRI-based estimation of the influence of brain tissue anisotropy on the effects of transcranial magnetic stimulation," *NeuroImage*, vol. 36, no. 4, pp. 1159–1170, 2007.

[11] W. H. Lee, Z. D. Deng, T. S. Kim, A. F. Laine, S. H. Lisanby, and A. V. Peterchev, "Regional electric field induced by electroconvulsive therapy: A finite element simulation study," in *Proceedings of the 32nd Annual International Conference of the IEEE Engineering in Medicine and Biology Society*, pp. 2045–2048, 2010.

[12] T. Oostendorp, Y. Hengeveld, C. Wolters, J. Stinstra, G. van Elswijk, and D. Stegeman, "Modeling transcranial DC stimulation," in *Proceedings of the 30th Annual International Conference of the IEEE Engineering in Medicine and Biology Society*, pp. 4226–4229, 2008.

[13] H. Suh, S. Kim, W. Lee, and T. Kim, "Realistic simulation of transcranial direct current stimulation via 3-d high-resolution finite element analysis: Effect of tissue anisotropy." in *Proceedings of the 31st Annual International Conference of the IEEE Engineering in Medicine and Biology Society*, pp. 638–641, 2009.

[14] D. Shattuck and R. Leahy, "BrainSuite: an automated cortical surface identification tool," *Medical Image Analysis*, vol. 6, no. 2, pp. 129–142, 2002.

[15] T. Behrens, M. Woolrich, M. Jenkinson, H. Johansen-Berg, R. Nunes, S. Clare, P. Matthews, J. Brady, and S. Smith, "Characterization and propagation of uncertainty in diffusion-weighted MR imaging," *Magnetic Resonance in Medicine*, vol. 50, no. 5, pp. 1077–1088, 2003.

[16] T. Behrens, H. Johansen-Berg, M. Woolrich, S. Smith, C. Wheeler-Kingshott, P. Boulby, G. Barker, E. Sillery, K. Sheehan, O. Ciccarelli, *et al.*, "Non-invasive mapping of connections between human thalamus and cortex using diffusion imaging," *Nature Neuroscience*, vol. 6, no. 7, pp. 750–757, 2003.

[17] T. Behrens, H. Berg, S. Jbabdi, M. Rushworth, and M. Woolrich, "Probabilistic diffusion tractography with multiple fibre orientations: What can we gain?" *NeuroImage*, vol. 34, no. 1, pp. 144–155, 2007.

[18] H. Johansen-Berg and T. Behrens, *Diffusion MRI: from quantitative measurement to in-vivo neuroanatomy*. Academic Press: London, UK, 2009.

[19] H. Hallez, B. Vanrumste, R. Grech, J. Muscat, W. De Clercq, A. Vergult, Y. D'Asseler, K. P. Camilleri, S. G. Fabri, S. Van Huffel, and I. Lemahieu, "Review on solving the forward problem in EEG source analysis," *Journal of NeuroEngineering and Rehabilitation*, vol. 4, no. 1, p. 46, 2007.

[20] M. Akhtari, H. C. Bryant, A. N. Mamelak, E. R. Flynn, L. Heller, J. J. Shih, M. Mandelkem, A. Matlachov, D. M. Ranken, E. D. Best, M. A. DiMauro, R. R. Lee, and W. W. Sutherling, "Conductivities of three-layer live human skull," *Brain Topography*, vol. 14, no. 3, pp. 151–167, 2002.

[21] S. B. Baumann, D. R. Wozny, S. K. Kelly, and F. M. Meno, "The electrical conductivity of human cerebrospinal fluid at body temperature," *IEEE Transactions on Biomedical Engineering*, vol. 44, no. 3, pp. 220–223, 1997.

[22] C. Gabriel, S. Gabriel, and E. Corthout, "The dielectric properties of biological tissues: I. Literature survey," *Physics in Medicine and Biology*, vol. 41, p. 2231, 1996.

[23] S. I. Gonçalves, J. C. de Munck, J. P. Verbunt, F. Bijma, R. M. Heethaar, and F. Lopes da Silva, "In vivo measurement of the brain and skull resistivities using an EIT-based method and realistic models for the head," *IEEE Transactions on Biomedical Engineering*, vol. 50, no. 6, pp. 754–767, 2003.

[24] S. Bai, C. Loo, and S. Dokos, "A computational model of direct brain stimulation by electroconvulsive therapy," in *Proceedings of the 32nd Annual International Conference of the IEEE Engineering in Medicine and Biology Society*, pp. 2069–2072, 2010.

[25] A. L. Hodgkin and A. F. Huxley, "A quantitative description of membrane current and its application to conduction and excitation in nerve," *Journal of Physiology*, vol. 117, no. 4, pp. 500–544, 1952.

[26] M. Nadeem, T. Thorlin, O. P. Gandhi, and M. Persson, "Computation of electric and magnetic stimulation in human head using the 3-D impedance method," *IEEE Transactions on Biomedical Engineering*, vol. 50, no. 7, pp. 900–907, 2003.

[27] H. Blumenfeld, M. Westerveld, R. B. Ostroff, S. D. Vanderhill, J. Freeman, A. Necochea, P. Uranga, T. Tanhehco, A. Smith, J. P. Seibyl, R. Stokking, S. C., S. S. Spencer, and I. G. Zubal, "Selective frontal, parietal, and temporal networks in generalized seizures," *NeuroImage*, vol. 19, no. 4, pp. 1556–1566, 2003.

[28] H. Blumenfeld, K. A. McNally, R. B. Ostroff, and I. George Zubal, "Targeted prefrontal cortical activation with bifrontal ECT," *Psychiatry Research: Neuroimaging*, vol. 123, no. 3, pp. 165–170, 2003.